

## Conference Paper

# Molecular Dynamics Simulations of Radiation Damage in Ti-Al based Structural Intermetallics

Roman Voskoboinikov

National Research Centre «Kurchatov Institute», Moscow, Russia

### Abstract

Molecular dynamics simulations were conducted to explore primary damage formation in collision cascades in  $\gamma$ -TiAl and  $\alpha_2$ -Ti<sub>3</sub>Al intermetallic compounds over a wide range of temperature  $100\text{K} < T < 900\text{K}$  and primary knock-on atom (PKA) energy  $5\text{keV} < E_{PKA} < 20\text{keV}$ . A series of 48 cascades for each  $(E_{PKA}, T)$  set was simulated to assure statistical reliability of the results. To quantify primary damage, the number of Frenkel pairs in the two intermetallic compounds was found as a function of  $(E_{PKA}, T)$  and compared with elemental metals.

It was established that Ti-Al based intermetallic compounds possess very high resistance against the formation of primary radiation defects. Understanding and controlling energy dissipation in irradiated intermetallic alloys may pave the way for new design concepts of radiation-tolerant structural and functional materials for nuclear engineering applications.

**Keywords:**  $\gamma$ -TiAl,  $\alpha_2$ -Ti<sub>3</sub>Al, intermetallic compounds, irradiation, molecular dynamics simulations, primary damage, Frenkel pairs, radiation resistance

Corresponding Author:  
 Roman Voskoboinikov  
 roman.voskoboinikov@gmail.com

Received: 21 December 2017  
 Accepted: 15 April 2018  
 Published: 6 May 2018

Publishing services provided by  
 Knowledge E

© Roman Voskoboinikov. This article is distributed under the terms of the [Creative Commons Attribution License](#), which permits unrestricted use and redistribution provided that the original author and source are credited.

Selection and Peer-review under the responsibility of the MIE-2017 Conference Committee.

## 1. INTRODUCTION

Raising economic and environmental sustainability of power engineering, transport and aerospace industry relies on the creation of new structural and functional materials capable of withstanding harsh operating conditions throughout the whole lifecycle without noticeable degradation of service properties. Despite significant efforts in the development of polymers, composite and ceramic structural materials, they are still far from being competitive with metals in most of demanding engineering applications. On the other hand, modern steels and alloys have been extensively developed over a past few decades and their capacity for ensuing improvements is nearly exceeded. Thus, further progress in the development of new breeds of energy conversion devices requires new materials that are built on qualitatively different physical principles. A

### OPEN ACCESS

number of research institutions and R&D divisions of commercial companies consider intermetallic alloys as a substitute to modern metallic systems in advanced engineering applications.

Due to unique combination of high specific strength and creep resistance, and stability of mechanical properties over a wide temperature range, Ti-Al based structural intermetallic alloys are considered as a substitute to heavier Ni-based refractory alloys in high temperature applications.  $\gamma$ -TiAl alloys have already been used for manufacturing low-pressure turbine blades of GEnx high-thrust turbofan jet engines to power modern Boeing 747-8 Intercontinental and Boeing 787 Dreamliner planes. Increasing the operating temperature of Ti-Al intermetallic alloys requires better oxidation and corrosion resistance that can be achieved by ion beam surface engineering. In order to optimize ion beam treatment of Ti-Al based intermetallic alloys for better performance it is essential to gain a deeper insight into radiation effects in these materials. From the fundamental perspective, Ti-Al intermetallic compounds represent a good model system for studying radiation effects in ordered metallic alloys for future nuclear engineering applications.

Collision cascades are the main source of radiation defects in materials subjected to fast particle irradiation in the nuclear stopping power regime. They are formed by the recoil of primary knock-on atoms (PKA) with the energy of more than  $\sim 1$  keV. The cascade process is characterized by the temporal and spatial scale of the order of  $\mu s$  and  $nm$ , respectively, which is prohibitive for direct experimental investigation but can be studied by molecular dynamics (MD) simulations.

In the present study, MD simulations were conducted to explore primary damage formation in collision cascades in  $\gamma$ -TiAl and  $\alpha_2$ -Ti<sub>3</sub>Al intermetallic compounds. The employed simulation techniques and approximations are described in the following section. The outcomes of the undertaken MD simulations are provided in the Results and Discussion part of the manuscript and the conclusions are drawn in the final section of the paper.

## 2. SIMULATION TECHNIQUE

Displacement of target atoms from their crystallographic positions in collision cascades is the primary process of the interaction of fast particles with crystalline solids exposed to irradiation in the nuclear stopping power regime. During the subsequent relaxation of the collision cascade region, most of the displaced atoms return to equilibrium

lattice sites whereas the remaining atoms occupy interstitial positions and form various interstitial configurations. Both self-interstitial atoms and vacancies can agglomerate into point defect clusters. Studying primary damage formation in the present research is reduced to MD simulations of collision cascades and evaluation of the number of residual point defects.

The semi-empirical interatomic potential [1] based on the embedded atom method (EAM) [2] is employed for evaluation of the interatomic forces in the simulated Ti-Al intermetallic compounds. The original interatomic potential [1] is not appropriate for studying radiation effects. In order to make it suitable for simulation of collision cascades, at short distances the pair part of Ti – Ti and Al – Al interatomic potentials was modified by fitting to the Biersack-Ziegler-Littmark universal repulsion potential [3, 4] following the procedure proposed in [5]. The experimentally measured threshold displacement energies for aluminium [6, 7] and  $\alpha$ -titanium [8, 9] were used as fitting parameters. The threshold displacement energies calculated using the modified interatomic potential are compared with available experimental data and simulation results, see Table 1 and the references cited therein for further details. The fitting procedure does not affect the equilibrium lattice parameters, the binding energies, the elastic constants, the vacancy formation energies, etc. of the elemental metals and intermetallic compounds.

TABLE 1: The threshold displacement energy  $E_d$ , eV, in elemental metals and intermetallic compounds.

Material and crystal structure	PKA	Crystallographic direction	$E_d$ , eV, present work	$E_d$ , eV, other studies	References
Al, fcc	Al	$\langle 110 \rangle$	$13 \leq E_d \leq 14$	$16 \pm 3$	[6, 7]
Ti, hcp	Ti	$\langle 11\bar{2}0 \rangle$	$19 \leq E_d \leq 20$	$19 \pm 1, 21 \pm 1$	[8, 9]
TiAl, $L_{10}$	Al	$\langle 110 \rangle$	$20 \leq E_d \leq 21$	16	[10]
TiAl, $L_{10}$	Ti	$\langle 110 \rangle$	$24 \leq E_d \leq 25$	20	[10]
TiAl, $L_{10}$	Al	$[101]$	$31 \leq E_d \leq 32$	$34 \pm 2, 20$	[9, 10]
TiAl, $L_{10}$	Ti	$[101]$	$24 \leq E_d \leq 25$	$28 \pm 2, 17$	[9, 10]
Ti <sub>3</sub> Al, $Do_{19}$	Al	$\langle 11\bar{2}0 \rangle$	$32 \leq E_d \leq 33$		
Ti <sub>3</sub> Al, $Do_{19}$	Ti	$[11\bar{2}0]$	$27 \leq E_d \leq 28$		
Ti <sub>3</sub> Al, $Do_{19}$	Ti	$[1\bar{2}10], [\bar{2}110]$	$21 \leq E_d \leq 22$		

Primary damage formation was studied in collision cascades initiated in  $\gamma$ -TiAl and  $\alpha_2$ -Ti<sub>3</sub>Al intermetallics with crystal structures  $L_{10}$  and  $Do_{19}$ , respectively, at four ambient temperatures  $T = 100, 300, 600$  and  $900$ K. By applying the virial theorem [11, 12], the

equilibrium lattice parameters were evaluated to fit the zero-pressure value for the selected simulation temperatures. The constant  $c/a$  ratios of 1.047 and 1.642 in  $\gamma$ -TiAl and  $\alpha_2$ -Ti<sub>3</sub>Al intermetallics, respectively, were used at all simulated temperatures. The equilibrium lattice parameters at different temperatures are given in Table 2.

TABLE 2: The equilibrium lattice parameters  $a$ , Å, in L<sub>10</sub> TiAl and Do<sub>19</sub> Ti<sub>3</sub>Al intermetallics at different temperatures.

Material	0K	100K	300K	600K	900K
L <sub>10</sub> TiAl	3,998	4,00411	4,01457	4,0327	4,053
Do <sub>19</sub> Ti <sub>3</sub> Al	2,892	2,8965	2,9038	2,9157	2,928

MD simulations of collision cascades were conducted at constant number of particles, constant volume and constant energy (*NVE* ensemble). MD box had close to cubic shape with {100} faces (in the case of  $\gamma$ -TiAl) or (1 $\bar{1}$ 00), (11 $\bar{2}$ 0) and (0001) faces (in the case of  $\alpha_2$ -Ti<sub>3</sub>Al). Periodic boundary conditions were applied at all faces.

Collision cascades were initiated by primary knock-on atoms (PKA) with PKA energy  $E_{PKA} = 5, 10, 15$  and 20 keV. During each execution, PKAs were introduced at different crystallographic positions along  $\langle 123 \rangle$  crystallographic direction at different moments of time in order to mimic the isotropic spatial and random temporal distribution of PKAs. A series of 48 collision cascades was simulated for each ( $E_{PKA}, T$ ) set of parameters. A half of the collision cascades in the series was initiated by aluminium PKAs, and the other half was initiated by titanium PKAs.

The size of MD cell was selected in accordance with the energy of PKA. The approximate number of mobile atoms in MD cells used in this study is provided in Table 3. MD cells were equilibrated at the selected simulation temperature for  $10^4$  MD iterations before PKA introduction. No temperature control/ dumping was applied during MD simulations of collision cascades. Typical change of the Maxwell temperature at different stages of relaxation of a 20 keV collision cascade is shown in Fig.1. The energy injected by a PKA was not extracted from the system. Temperature increase after the relaxation of a collision cascade region does not exceed  $\approx 40^\circ$  in any of the simulations.

TABLE 3: The approximate number of atoms  $N$  in MD simulation box that we used for simulation of collision cascades initiated by PKAs with different energies.

$E_{PKA}$	5 keV	10 keV	15 keV	20 keV
$N$	$5 \times 10^5$	$1 \times 10^6$	$1.5 \times 10^6$	$2 \times 10^6$

During the initial stage of a collision cascade, a small fraction of target atoms is moving with high velocities whereas the rest of the simulated crystal remains in the state of

the thermodynamic equilibrium at the selected simulation temperature. Because the convergence of the velocity-Verlet algorithm [11] that is applied in this study depends on the time step  $\tau$  evaluated in accordance with the energy of the fastest atom, direct integration of the equations of motion of all atoms in the MD cell would lead to a nonoptimal use of high performance computing (HPC) resources. In order to facilitate calculations and optimise utilisation of HPC facilities, the methodology proposed in [14] is implemented. Energy conservation and the effectiveness of the algorithm based on [14] were tested earlier, and the algorithm itself was employed for MD simulations of radiation damage in copper [15],  $\alpha$ -zirconium [16, 17] and studying the interaction of collision cascades with dislocations [18, 19].

Three different techniques, namely the Lindemann spheres [20], the Wigner-Seitz cell analysis [21, 22] and cluster analysis [15] were applied to identify residual point defects created in collision cascades. The threshold radius of  $0.3a$ , where  $a$  is the equilibrium lattice parameter, was used in the Lindemann spheres, and the radius of the first coordination sphere was used for point defect cluster identification in cluster analysis.

### 3. RESULTS AND DISCUSSION

The number of Frenkel pairs  $N_{FP}$  produced in collision cascades is the key characteristic that determines both the radiation tolerance of structural materials and the whole range of radiation-induced and radiation-assisted phenomena. The number of Frenkel pairs in  $\gamma$ -TiAl and  $\alpha_2$ -Ti<sub>3</sub>Al intermetallics is shown in Figures 2 and 3, respectively, as a function of PKA energy and crystal temperature. Figures 2a and 3a contain the information about collision cascades initiated in  $\gamma$ -TiAl and  $\alpha_2$ -Ti<sub>3</sub>Al intermetallics by aluminium PKAs, whereas Figures 2b and 3b retain the outcome of MD simulations of collision cascades in  $\gamma$ -TiAl and  $\alpha_2$ -Ti<sub>3</sub>Al intermetallics initiated by titanium PKAs. Each open symbol in Figures 2 and 3 corresponds to the number of Frenkel pairs created in one cascade. The average number of Frenkel pairs,  $\langle N_{FP} \rangle$ , is shown with solid symbols.

Despite a noticeable difference in the threshold displacement energy  $E_d$  of aluminium and titanium atoms in the two intermetallic compounds, see Table 1, the average number  $\langle N_{FP} \rangle$  and the functional form of  $\langle N_{FP}(E_{PKA}, T) \rangle$  do not depend on the PKA type. A simple explanation of this effect is connected with the size of a cascade region. Since the number of displaced atoms in a collision cascade is of the order of a few thousands, see the example in Figure 1, PKA energy is transferred to many

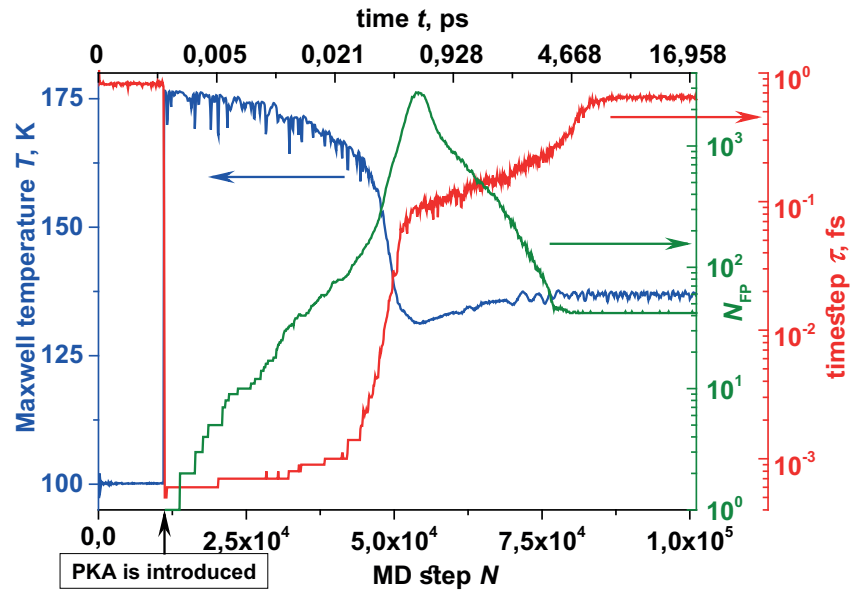


**Figure 1:** Maxwell temperature  $T$ , time step  $\tau$  and the number of displaced atoms  $N_{FP}$  at different stages of relaxation of a 20 keV collision cascade in  $\gamma$ -TiAl at 100K.

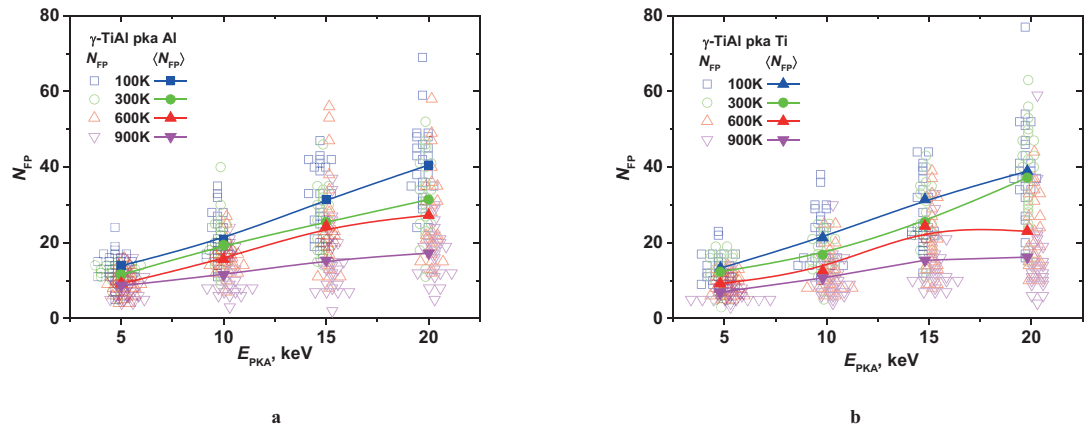


**Figure 2:** The number of Frenkel pairs  $N_{FP}$  created in collision cascades in  $\gamma$ -TiAl as a function of  $(E_{PKA}, T)$ . Each scatter point corresponds to  $N_{FP}$  produced in one collision cascade. The average number of Frenkel pairs  $\langle N_{FP} \rangle$  generated in a series of collision cascades with the same  $(E_{PKA}, T)$  set is shown with solid symbols. The outcomes of MD simulations of collision cascades initiated by aluminium and titanium PKAs are shown in figures a and b, respectively.

secondary, tertiary, ... etc. titanium and aluminium knock-on atoms, and the type of the first displaced atom is not essential anymore.

The spread of the number of Frenkel pairs created in collision cascades in the two intermetallic compounds under the same simulation conditions is wide, see Figures 2 and 3. The dispersion increases with the increase of  $E_{PKA}$  and the decrease of  $T$ . In order to get the statistically reliable number of Frenkel pairs, we need to evaluate the optimal sampling size. A simple procedure is proposed to serve this purpose. In the undertaken research, the dependence of the average number of Frenkel pairs  $\langle N_{FP} \rangle$  is

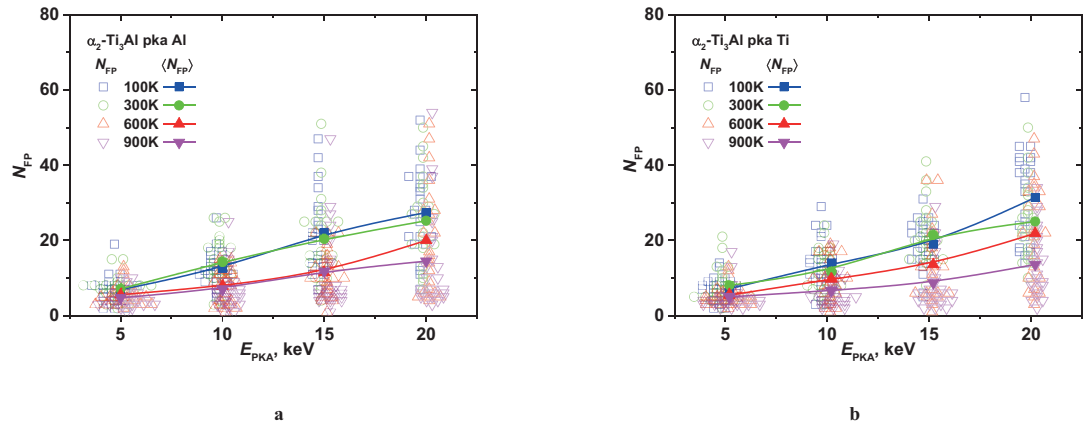


**Figure 3:** The number of Frenkel pairs  $N_{FP}$  created in collision cascades in  $\alpha_2$ -Ti<sub>3</sub>Al as a function of  $(E_{PKA}, T)$ . Each scatter point corresponds to  $N_{FP}$  produced in one collision cascade. The average number of Frenkel pairs  $\langle N_{FP} \rangle$  generated in a series of collision cascades with the same  $(E_{PKA}, T)$  set is shown with solid symbols. The outcomes of MD simulations of collision cascades initiated by aluminium and titanium PKAs are shown in Figures a and b, respectively.

built for all MD simulation conditions as a function of the sampling size  $n$ .  $\langle N_{FP} \rangle$  vs the number of collision cascades in a series with the same  $(E_{PKA}, T)$  is shown in Figures 4 and 5 for the case of  $E_{PKA} = 20\text{keV}$  in  $\gamma$ -TiAl and  $\alpha_2$ -Ti<sub>3</sub>Al intermetallic compounds, respectively. The Figures demonstrate saturation of the average number of Frenkel pairs  $\langle N_{FP} \rangle$  with the increase of the sampling size. Apparently, more than 42 collision cascades in a series with the same  $(E_{PKA}, T)$  set is necessary in order to get the correct number of  $\langle N_{FP} \rangle$  for quantitative description of the formation of primary damage in  $\gamma$ -TiAl. Similarly, a series of MD simulations of at least 36 collision cascades with the same  $(E_{PKA}, T)$  set is required in order to evaluate the statistically reliable dependence  $\langle N_{FP}(E_{PKA}, T) \rangle$  in  $\alpha_2$ -Ti<sub>3</sub>Al.

Primary damage formation in elemental metals and their alloys has been extensively studied by MD simulations over a few decades. It was established that the average number of Frenkel pairs has no obvious dependence on the crystal structure or other physical properties. The only difference in  $\langle N_{FP} \rangle$  that does exist between metals and alloys appear to be solely due to the average atomic mass of the target, for  $\langle N_{FP} \rangle$  is highest in light metals [23]. Nevertheless, the undertaken research clearly demonstrates that primary damage formation in the two studied Ti-Al based intermetallic compounds does not comply with that observation.

Following [23], a comparison of  $\langle N_{FP} \rangle$  created in 20 keV collision cascades in several materials at different temperatures is provided in Figure 6. The average number of Frenkel pairs produced in collision cascade both in  $\gamma$ -TiAl and  $\alpha_2$ -Ti<sub>3</sub>Al is significantly lower than predicted on the ground of the average atomic mass of these intermetallic

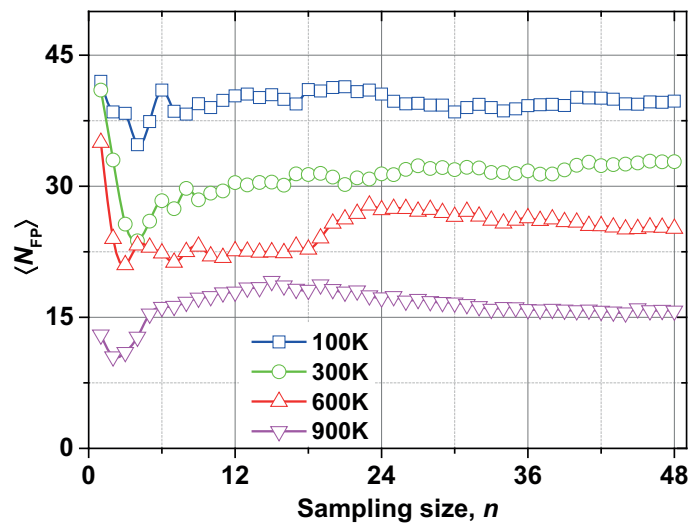


**Figure 4:** Dependence of the average number of Frenkel pairs  $\langle N_{FP} \rangle$  created in 20 keV collision cascades in  $\gamma$ -TiAl as a function of the sampling size  $n$ .

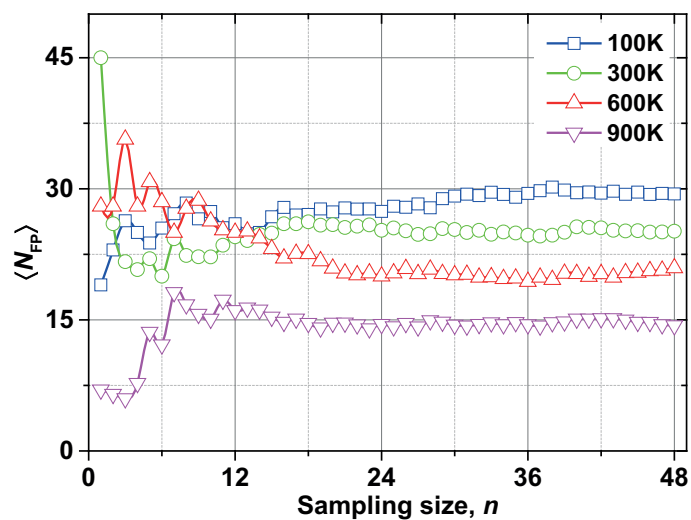


**Figure 5:** Dependence of the average number of Frenkel pairs  $\langle N_{FP} \rangle$  created in 20 keV collision cascades in  $\alpha_2$ -Ti<sub>3</sub>Al as a function of the sampling size  $n$ .

compounds. High resistance of the intermetallic compounds against the formation of primary damage can be attributed to a mixed nature of metallic and covalent bonding or the ordered character of their crystal structures with intrinsic antisite point defects or both. A deeper insight into the physical mechanisms of high radiation tolerance of intermetallic compounds is required.



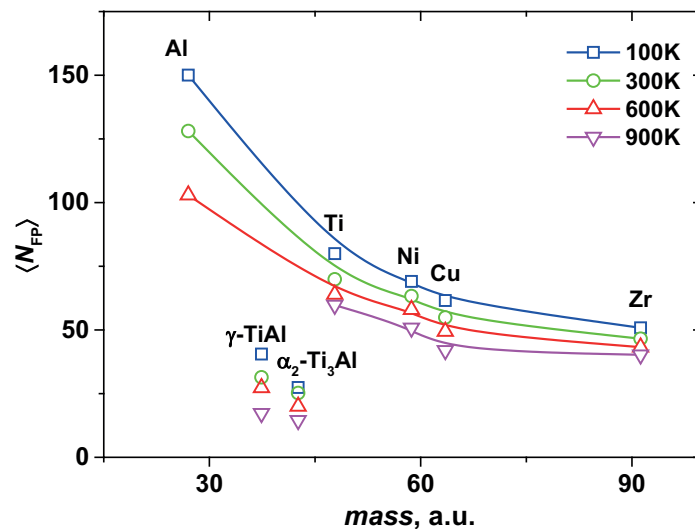


**Figure 6:** The average number of Frenkel pairs  $\langle N_{FP} \rangle$  produced in 20keV cascades in elemental metals and intermetallic compounds at different temperatures as a function of the average atomic mass of the target.

## 4. CONCLUSION

More than 1900 displacement cascades were simulated in  $\gamma\text{-TiAl}$  and  $\alpha_2\text{-Ti}_3\text{Al}$  intermetallic compounds over a wide range of temperature,  $100\text{K} < T < 900\text{K}$ , and PKA energy,  $5\text{keV} < E_{PKA} < 20\text{keV}$ . The average number of Frenkel pairs  $\langle N_{FP} \rangle$  was evaluated in the two intermetallic compounds as a function of  $(E_{PKA}, T)$ . A simple routine has been suggested to justify the statistical reliability of the obtained quantitative results.

No channelling events were observed under all simulation conditions.

It was established that both  $\gamma\text{-TiAl}$  and  $\alpha_2\text{-Ti}_3\text{Al}$  possess high radiation tolerance. Understanding and controlling energy dissipation in intermetallic compounds exposed to fast particle irradiation in the nuclear stopping power regime may pave the way for new design principles of radiation-tolerant structural and functional materials suitable for future nuclear engineering applications.

## ACKNOWLEDGEMENT

The undertaken research was conducted under partial support from the Russian Foundation for Basic Research, grant RFBR 17-03-01222a. MD simulations were carried out using computing resources of the Complex for Simulation and Data Processing for Mega-science Facilities at NRC Kurchatov Institute, <http://ckp.nrcki.ru/>.

## DECLARATION OF COMPETING INTERESTS

The author declares no affiliations with or involvement in any organisation or entity with any financial or non-financial interest in the subject matter or materials discussed in this research paper.

## References

- [1] R.R. Zope, Y. Mishin, *Phys. Rev. B* 68 (2003) 024102-14
- [2] M.S. Daw, M.I. Baskes, *Phys. Rev. B* 29 (1984) 6443-6453
- [3] J.P. Biersack, J.F. Ziegler, *Nucl. Instr. Meth. Phys. Res.* 194 (1982) 93-100
- [4] J.F. Ziegler, J.P. Biersack, U. Littmark, *The Stopping and Range of Ions in Solids*, Pergamon Press, New York, 1985, 321p
- [5] K. Gärtner, D. Stock, B. Weber, G. Betz, M. Hautala, G. Hobler, M. Hou, S. Sarite, W. Eckstein, J.J. Jiménez-Rodríguez, A.M.C. Pérez-Martín, E.P. Andribet, V. Konoplev, A. Gras-Marti, M. Posselt, M.H. Shapiro, T.A. Tombrello, H.M. Urbassek, H. Hensel, Y. Yamamura, W. Takeuchi, *Nucl. Instr. Meth. Phys. Res. B* 102 (1995) 183-197
- [6] H.I. Dawson, G.W. Iseler, A.S. Mehner, J.W. Kauffman, *Phys. Lett.* 18 (1965) 247-248
- [7] G.W. Iseler, H.I. Dawson, A.S. Mehner, J.W. Kauffman, *Phys. Rev.* 146 (1966) 468-471
- [8] C.G. Shirley, R.L. Chaplin, *Phys. Rev. B* 5 (1972) 2027-2029
- [9] G. Sattonnaya, F. Rullier-Albenque, O. Dimitrova, *J. Nucl. Mater.* 275 (1999) 63-73
- [10] B.-Y. Wang, Y.-X. Wang, Q. Gu, T.-M. Wang, *Comput. Mater. Sci.* 8 (1997) 267-272
- [11] L.D. Landau, E.M. Lifshitz, *Mechanics, Third Edition: Volume 1 (Course of Theoretical Physics 5)*, Butterworth-Heinemann; 1976, 224p
- [12] V.A. Fock, *Fundamentals of Quantum Mechanics*, Mir Publishers, 1978, 367p
- [13] M.P. Allen, D.J. Tildesley, *Computer Simulation of Liquids*. Clarendon Press, Oxford, 1987, 408p
- [14] L.A. Marques, J.E. Rubio, M. Jaraiz, L. Enriquez, J. Barbolla, *Nucl. Instr. Meth. Phys. Res. B* 102 (1995) 7-11
- [15] R.E. Voskoboinikov, Yu.N. Osetsky, D.J. Bacon, *J. Nucl. Mater.* 377 (2008) 385-395
- [16] R.E. Voskoboinikov, Yu.N. Osetsky, D.J. Bacon, *Journal of ASTM International* 2 (2005)12419-1-15
- [17] R.E. Voskoboinikov, Yu.N. Osetsky, D.J. Bacon *ASTM STP1475* (2006) 299-314
- [18] R.E. Voskoboinikov *Nucl. Instr. Meth. Phys. Res. B* 303 (2013) 104-107

- [19] R.E. Voskoboinikov Nucl. Instr. Meth. Phys. Res. B 303 (2013) 125-128
- [20] F.A. Lindemann Zeitschrift für Physik 11 (1910) 609-612
- [21] K. Nordlund, R.S. Averback, Phys. Rev. B 56 (1997) 2421-2431
- [22] [https://ovito.org/manual/particles.modifiers.wigner\\_seitz\\_analysis.html](https://ovito.org/manual/particles.modifiers.wigner_seitz_analysis.html)
- [23] D.J. Bacon, F. Gao and Yu.N. Osetsky, J. Nucl. Mater. 276 (2000) 1-12